Chapter 1
Advances in 4D Gated Cardiac PET Imaging for Image Quality Improvement and Cardiac Motion and Contractility Estimation

Benjamin M.W. Tsui, Tao Feng, Jizhe Wang, Jingyan Xu, M. Roselle Abraham, Stefan L. Zimmerman, and Thomas H. Schindler

Abstract Quantitative four-dimensional (4D) image reconstruction methods with respiratory and cardiac motion compensation are an active area of research in ECT imaging, including SPECT and PET. They are the extensions of three-dimensional (3D) statistical image reconstruction methods with iterative algorithms that incorporate accurate models of the imaging process and provide significant improvement in the quality and quantitative accuracy of the reconstructed images as compared to that obtained from conventional analytical image reconstruction methods. The new 4D image reconstruction methods incorporate additional models of the respiratory and cardiac motion of the patient to reduce image blurring due to respiratory motion and image noise of the cardiac-gated frames of the 4D cardiac-gated images. We describe respiratory motion estimation and gating method based on patient PET list-mode data. The estimated respiratory motion is applied to the respiratory gated data to reduce respiratory motion blur. The gated cardiac images derived from the list-model data are used to estimate cardiac motion. They are then used in the cardiac-gated images summing the motion-transformed cardiac-gated images for significant reduction in the gated images noise. Dual respiratory and cardiac motion compensation is achieved by combining the respiratory and cardiac motion compensation steps. The results are further significant improvements of the 4D gated cardiac PET images. The much improved gated cardiac PET image quality increases the visibility of anatomical details of the heart, which can be explored to provide more accurate estimation of the cardiac motion vector field and cardiac contractility.

Keywords 4D gated cardiac PET • 4D image reconstruction methods • Respiratory and cardiac motion estimation and compensation

B.M.W. Tsui (✉) • T. Feng • J. Wang • J. Xu • S.L. Zimmerman • T.H. Schindler
Department of Radiology, Johns Hopkins Medical Institute, Baltimore, MD, USA
e-mail: btsui1@jhmi.edu

M.R. Abraham
Department of Medicine, Johns Hopkins Medical Institute, Baltimore, MD, USA

Y. Kuge et al. (eds.), *Perspectives on Nuclear Medicine for Molecular Diagnosis and Integrated Therapy*, DOI 10.1007/978-4-431-55894-1_1

1.1 Introduction

The development of quantitative image reconstruction in medical imaging, including emission computed tomography (ECT) and x-ray CT [1, 2], has recently shifted from three-dimensional (3D) to four-dimensional (4D), i.e., the inclusion of the time dimension. There are two major goals for this development. First is to reduce reconstructed image artifacts due to patient motion. In particular, compensation of involuntary patient motion, e.g., respiratory motion, that causes resolution loss has received much attention [3–6]. Second is to improve the temporal resolution of dynamic images for improved detection of global and regional motion abnormalities [7, 8]. An important application is gated myocardial perfusion (MP) ECT imaging. Despite extensive research in other imaging modalities over the last two decades, MP ECT, especially gated SPECT and more recently PET, has continued to be the major biomedical imaging technique for the assessment of MP in clinical practice. The potential of extracting additional quantitative information, such as abnormalities from existing data without additional clinical studies, radiation dose or discomfort to the patients, has great significance in biomedical imaging [9–13].

The long-term goal of the study is to integrate the two aforementioned goals of the current quantitative 4D imaging reconstruction methods, i.e., to improve the quality and quantitative accuracy of the 4D cardiac gated MP PET images while reducing the blurring caused by respiratory motion (RM) and cardiac motion (CM). This is in addition to compensation of other image degrading factors, e.g., statistical noise, photon attenuation and scatter, and collimator-detector blur, to improve both spatial and temporal resolution. In this work, we present the development of a data-driven RM estimation method and quantitative 4D statistical image reconstruction methods that compensate for RM and CM separately, and for dual respiratory and cardiac (R&C) motion for improved lung and cardiac PET imaging. We hypothesize that by applying a statistical 4D image reconstruction method that accurately compensates for RM and CM and other image degrading factors, we would be able to minimize image artifacts caused by the image degrading factors, improve image resolution and reduce image noise. This would result in two significant clinical benefits, i.e., (a) reduction of false positives and false negatives for improved diagnosis, and (b) reduction of imaging time and/or radiation dose to the patient.

In addition, the much improved 4D gated cardiac PET image quality increases the visibility of details of cardiac structures. The information can be explored in a feature-based motion estimation method to determine the cardiac motion vector field and cardiac contractility.

1.2 Materials and Methods

1.2.1 Data-Driven Respiratory Motion Detection and Gating Method

There are two general approaches to obtain respiratory gated PET data [14]. One is to use an external tracking device that directly measures a RM surrogate [3, 15]. The other is to derive RM information from the acquired data [16–19]. These data-driven RM detection methods can avoid the cost and effort and directly provide a surrogate RM signal. We developed two data-driven methods that estimated the RM from $^{13}NH_3$ and ^{18}F-FDG cardiac gated list-mode PET data. In Fig. 1.1a, b, the $^{13}NH_3$ images show more liver uptake than the ^{18}F-FDG images. Our data-driven method for the $^{13}NH_3$ was based on the total counts in each consecutive short segment (200–500 ms) of PET data. For the ^{18}F-FDG, RM signal was extracted based on the axial center-of-mass of the short segment PET data. Figure 1.1c shows the relative RM gating signal amplitude as a function of time obtained from the $^{13}NH_3$ list-mode data. The estimated RM signal compared well with that obtained from an external tracking device. It was used to divide the RM into multiple respiratory gates. The respiratory gated image data were used to estimate the motion vector field of the RM and incorporated in the 4D image reconstruction method to achieve motion compensation.

From the estimated RM signal in Fig. 1.1c, we divided the list-mode data into six equal-count respiratory frames, each of which is further divided into eight cardiac-gated frames using the ECG R-wave markers. The result was a full set of dual six-frame respiratory gated and eight-frame cardiac-gated dataset. We then applied the RM compensation method described in Sect. 1.2 to the six-frame respiratory-gated dataset.

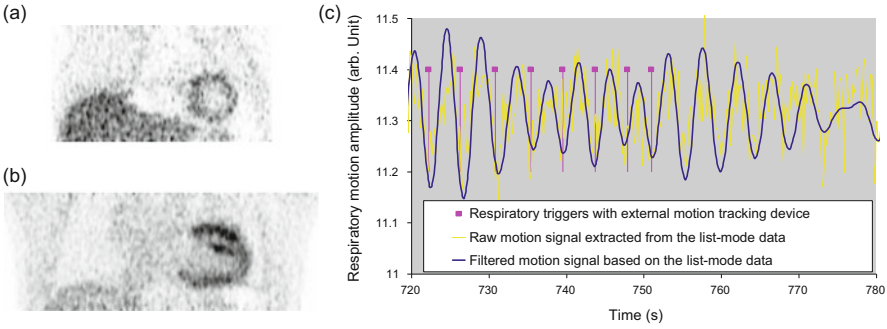

Fig. 1.1 Sample respiratory-gated projection images from (**a**) $^{13}NH_3$ cardiac and (**b**) ^{18}F-FDG cardiac images. (**c**) Comparison of a RM signal derived from an external tracking device and from the total count variation of the short segment projections of the $^{13}NH_3$ cardiac PET data

1.2.2 4D PET Image Reconstruction Methods with Attenuation, and Respiratory and Cardiac Motion Compensation

The 4D PET image reconstruction methods used in this study were applied to the respiratory-gated and cardiac-gated projection data. Specifically, for the 4D PET image reconstruction method with dual R&C motion compensation, we divided the acquired list-mode data into six equal-count respiratory frames each with eight cardiac-gated frames as described in Sect. 1.2.1. Image reconstructions without attenuation correction were performed on this dataset to estimate the RM in lung PET studies and both RM and CM in cardiac PET studies. A special feature of our method was the modeling of the RM-induced deformations of the PET image and CT-based attenuation map in RM estimation and during PET image reconstruction for accurate and artifact-free attenuation corrected PET images.

1.2.2.1 4D PET Image Reconstruction with Respiratory Motion and Attenuation Compensation

We developed a 4D PET image reconstruction method with RM and attenuation compensation to improve the image quality of ^{18}F-FDG PET images for improved small lung lesion detection [20, 21]. First, a reference respiratory gated frame was chosen from the six equal-count respiratory frames. Then the PET image at the reference frame and the RM from the reference frame to the other respiratory-gated PET frames were estimated by minimizing the Poisson log-likelihood function. As shown in Fig. 1.2, the RM-induced deformations of both the PET image and CT-based attenuation map were modeled in the RM estimation and during PET image reconstruction. Our method is applicable to respiratory-gated PET data from current clinical PET/CT imaging procedures with only one CT-based attenuation map. We solved the image reconstruction problem in two steps: (1) estimated the RM using an iterative approach, and (2) modeled the estimated RM in a 4D OS-EM image reconstruction algorithm [21] that achieved 6 ~ 10 times acceleration over the 4D ML-EM algorithms proposed by others [22, 23]. The final estimated RM-induced deformations were applied to transform and registered all the respiratory gated frame images to the reference frame. The corresponding eight cardiac-gated frames from within the transformed respiratory-gated frames were summed resulting in the eight cardiac-gated image with respiratory compensation, that is, without RM blurring effect.

In a practical implementation of the above method [24], the RM was estimated from the 4D respiratory- gated PET images obtained without attenuation correction. The estimated RM was used in the 4D image reconstruction shown in Fig. 1.2 without further update. It provided respiratory-gated attenuation effect that matches the respiratory-gated PET images for accurate attenuation compensation.

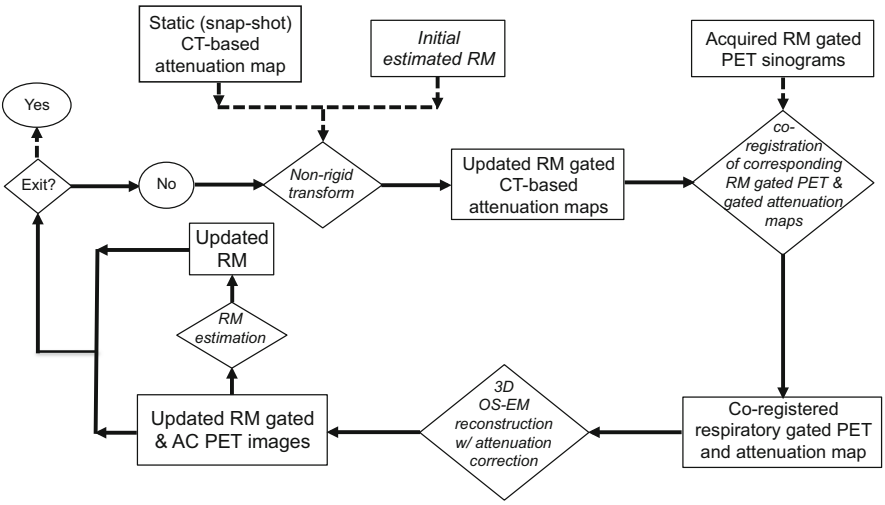

Fig. 1.2 A flowchart of the 4D image reconstruction method with RM and attenuation compensation. A snap-shot CT image was acquired from which a static attenuation map was derived. A reference respiratory gated frame was chosen. The updated PET image at the reference frame and the RM from the reference frame to the other respiratory-gated PET frames were jointly estimated by minimizing the log-likelihood function

1.2.2.2 4D Image Reconstruction with Cardiac Motion Compensation

In CM compensation, a reference frame was chosen from the eight-frame cardiac-gated images. As shown in Fig. 1.3, a B-spline non-rigid transformation and registration was applied to each cardiac-gated image and registered it to the reference frame and summed. The procedure was repeated at different cardiac-gated frames in the cardiac cycle to form the CM compensated gated cardiac image set.

1.2.2.3 4D Image Reconstruction with Dual Respiratory and Cardiac Motion Compensation

The 4D image reconstruction with dual R&C motion compensation was achieved by combining the RM and CM compensation described in Sects. 1.2.2.1 and 1.2.2.2. After estimating the accurate RM and respiratory gated attenuation maps based on Sect. 1.2.2.1, 48-frame dual R&C gated images were obtained. For each cardiac gate, the RM compensation described in Sect. 1.2.2.1 was used. The result was RM compensated cardiac-gated images. Cardiac motion compensation was achieved by applying the same approach in Sect. 1.2.2.2. The resultant eight-frame gated cardiac images shown in Fig. 1.3 thus included both RM and CM compensation.

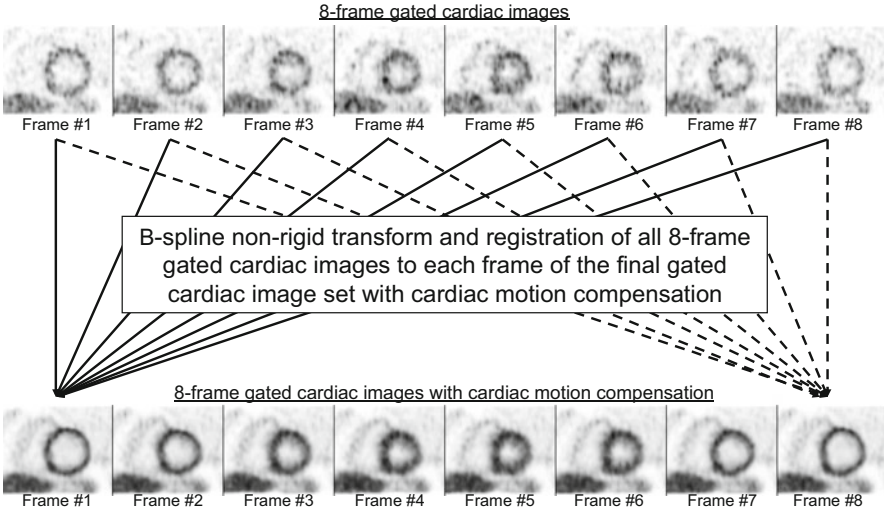

Fig. 1.3 In the CM compensation, a B-spline non-rigid transformation and registration was applied to each cardiac-gated image and registered it to the reference frame and summed

1.2.3 Evaluation of the 4D PET Image Reconstruction with Respiratory and Attenuation Compensation

We evaluated the 4D image reconstruction method with respiratory and attenuation compensation to two clinical applications. They were the detection of small lung lesions and the improvement of image quality in gated cardiac PET images. In the lung lesion detection study, we used realistic simulated 4D respiratory gated lung PET projection data. In the gated cardiac study, patient data from a $^{13}NH_3$ MP PET study and a ^{18}F-FDG cardiac PET study were used. The goal was to assess the reduction of image resolution from blurring due to RM.

1.2.3.1 Evaluation Using Realistic Simulated PET Study with Small Lung Lesions

We evaluated the 4D PET image reconstruction with respiratory and attenuation compensation method using a realistic Monte Carlo (MC) simulated PET dataset from the 4D XCAT (eXtended CArdiac Torso) phantom [25]. The 4D XCAT phantom is an extension of the 4D NCAT (Nurbs-based CArdiac Torso) phantom [26], which provides realistic models of the anatomical structures of the entire human body based on the visible human data [27]. In addition, the 4D XCAT phantom includes realistic models of normal RM based on respiratory-gated CT data [28], and normal cardiac motion based on tagged MRI data. The cardiac motion model in the new 4D XCAT is based on state-of-the-art high-resolution

cardiac-gated CT and tagged MRI data [29]. A 4D activity distribution phantom that modeled the uptake of the PET tracer in the different organs and a corresponding 4D attenuation coefficient distribution phantom that modeled the attenuation of different organs at the 511 keV photon energy were generated based on the 4D XCAT phantom. In addition, three small lung lesions with increased activity uptakes were inserted at different locations in the lung. The 4D activity distribution also served as the truth in the quantitative evaluation study.

Realistic respiratory-gated PET projection data were generated from the 4D activity and attenuation distributions using a combined SimSET [30] and GATE [31] MC simulation software that took advantage of the high efficiency of the former in computing the photon transport in the voxelized phantom and the ability of the latter to model the complex detector geometry and imaging characteristics of a clinical GE PET system [32]. The 4D PET image reconstruction method with RM and attenuation compensation was applied to the simulated RM-gated projection data. The results were compared to those obtained with conventional 3D and 4D image reconstruction methods without motion compensation.

1.2.3.2 Evaluation Using Data from Clinical Gated Cardiac PET Studies

We also evaluated the clinical efficacy of the 4D image reconstruction method with RM and attenuation compensation using clinical $^{13}NH_3$ MP PET and ^{18}F-FDG cardiac PET data. A GE Discovery VCT (RX) PET/CT system was used in the patient studies. Prior to the PET scan, a low-dose CT scan was acquired from the patient. In the $^{13}NH_3$ MP PET study, ~370 MBq of $^{13}NH_3$ was infused intravenously as a bolus over 10 s. List-mode PET data were acquired for 20 min. In the ^{18}F-FDG cardiac PET study of a different patient, ~370 MBq of ^{18}F-FDG was administered through IV injection. A list-mode PET data acquisition was performed ~60 min post injection. The 4D image reconstruction method with RM and attenuation compensation as described in Sect. 1.2.1 were applied to the acquired list-mode data. The resultant MP PET and cardiac PET images were compared to those obtained with the conventional image reconstruction method without RM compensation. Specifically, they were evaluated for improved lung lesion detection from the reduction of resolution loss due to RM blur.

1.2.4 Evaluation of the 4D PET Image Reconstruction Method with Dual Respiratory and Cardiac Motion Compensation

The evaluation of the 4D PET image reconstruction method with dual R&C motion compensation was performed on the same clinical $^{13}NH_3$ MP PET and ^{18}F-FDG

cardiac PET datasets used in Sect. 1.2.3.2. Here, the goal was to assess the improvement of the quality of the gated cardiac PET images in terms of image resolution and image noise.

1.3 Results and Discussion

1.3.1 Improvement of Small Lung Lesion Detection with Respiratory and Attenuation Compensation

We evaluated the 4D PET image reconstruction with respiratory and attenuation compensation method using a realistic simulated PET dataset from the 4D XCAT phantom [19, 20] and the Monte Carlo (MC) method as described in Sect. 1.2.3. The method included RM detection using the data-driven gating method as described in Sect. 1.2.1. The results are shown in Fig. 1.4. The activity distribution of the 4D XCAT phantom with three small lung lesions is shown in Fig. 1.4a. The reconstructed PET images without RM compensation in Fig. 1.4b show the resolution loss due to RM blur. Also the reconstructed images with RM and attenuation compensation using the known RM from the 4D XCAT phantom (Fig. 1.4c) and using the estimated RM (Fig. 1.4d) were compared. The results indicate the effectiveness of the RM estimation method and the 4D image reconstruction

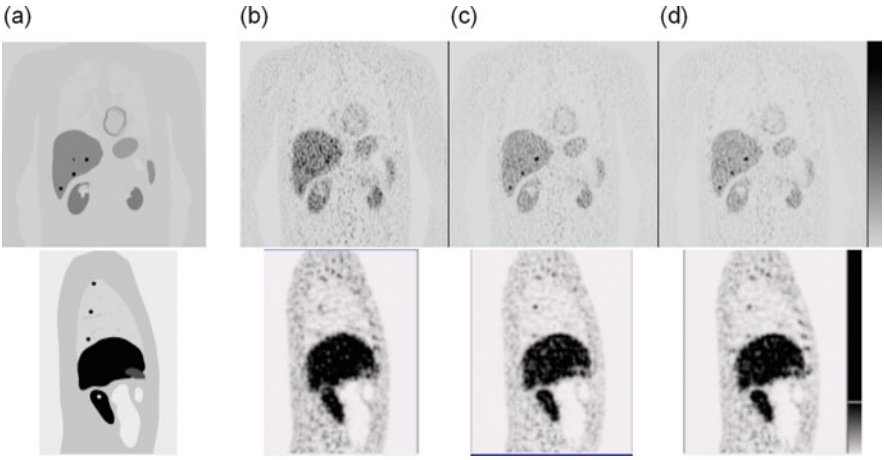

Fig. 1.4 Results from a simulation study to evaluate the 4D PET image reconstruction with respiratory and attenuation compensation for improved lung lesion detection. A realistic MC simulated PET dataset from the 4D XCAT phantom was used. A sample (*Top row*) coronal slice and (*Bottom row*) sagittal slice through the lung showing three small lung nodules. (**a**) Activity distribution of the 4D XCAT phantom. Reconstructed images obtained from using (**b**) the 3D ML-EM method with no RM compensation, and the 4D ML-EM method (**c**) with modeling of the true RM from the 4D XCAT phantom, and (**d**) with the RM estimation described in Sect. 1.2.1

method with RM and attenuation compensation to reduce resolution loss due to RM blur and to improve small lung lesion detection in lung PET images.

1.3.2 Improvement of Gated Cardiac PET Images with Respiratory Motion and Attenuation Compensation

We applied the 4D image reconstruction method with RM and attenuation compensation to the clinical $^{13}NH_3$ MP PET and ^{18}F-FDG cardiac PET datasets described in Sect. 1.2.3.2. The results are shown in Figs. 1.5 and 1.6, respectively. Figures 1.5a

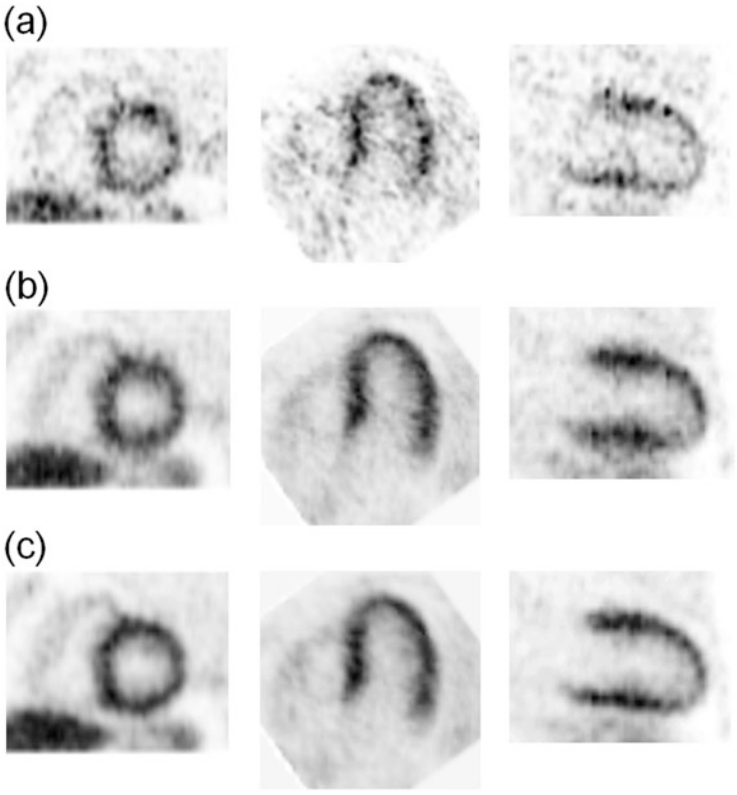

Fig. 1.5 (**a**) Sample images from one of the six respiratory-gated frames and from selected sample (*Left*) short-axis, (*Middle*) horizontal long-axis, and (*Right*) vertical long-axis slice images obtained using a 3D OS-EM image reconstruction without any motion compensation from a $^{13}NH_3$ MP PET study. (**b**) The sum of all six respiratory gated images from (a) showing the effect of RM blur. (**c**) Corresponding sample images as in (b) obtained using the 4D OS-EM image reconstruction with RM and attenuation compensation showing the reduction of RM motion blur in the reconstructed images

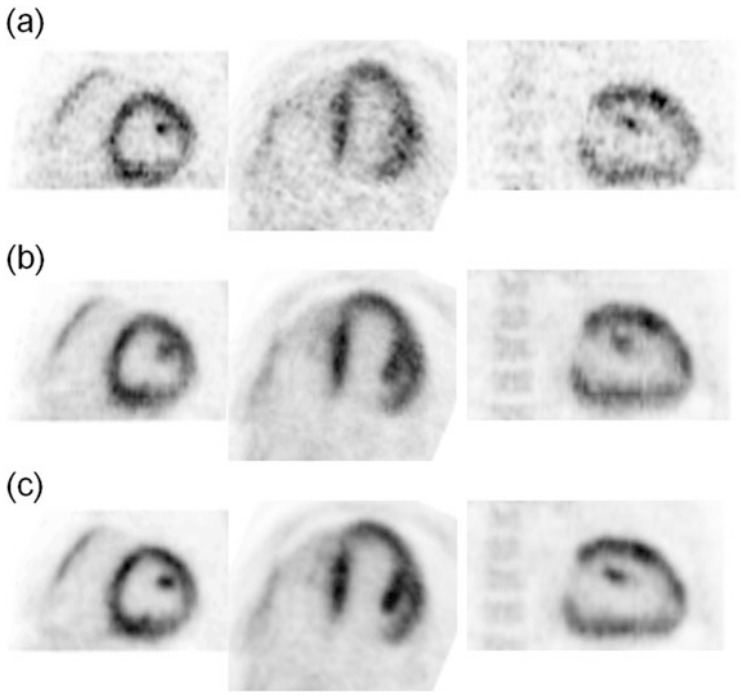

Fig. 1.6 (**a**) Sample images from one of the six respiratory-gated frames and from selected sample (*Left*) short-axis, (*Middle*) horizontal long-axis, and (*Right*) vertical long-axis slice images obtained using a 3D OS-EM image reconstruction without any motion compensation from a ^{18}F-FDG cardiac PET study. (**b**) The sum of all six respiratory-gated frames from (a) showing the effect of RM blur. (**c**) Corresponding sample images as in (b) obtained using the 4D OS-EM image reconstruction with RM and attenuation compensation showing the reduction of RM motion blur in the reconstructed images

and 1.6a are sample images from one of the six respiratory-gated frames and from selected sample short-axis, horizontal long-axis, and vertical long-axis slice images obtained using a 3D OS-EM image reconstruction without any motion compensation are shown. Figures 1.5b and 1.6b are the sum of all six respiratory-gated frame images demonstrating the effect of RM blur. The corresponding images obtained using the 4D OS-EM image reconstruction with RM and attenuation compensation are shown in Figs. 1.5c and 1.6c. They show the reduction of RM motion blur in the reconstructed images.

1.3.3 Improvement of Gated Cardiac PET Images with Dual Respiratory and Cardiac Motion Compensation

We applied the 4D image reconstruction method with dual R&C motion compensation to the clinical $^{13}NH_3$ MP PET and ^{18}F-FDG cardiac PET datasets described in Sect. 1.2.3.2. The results are shown in Figs. 1.7 and 1.8, respectively. Figures 1.7a and 1.8a and sample images from one of the eight cardiac-gated frames and from selected sample short-axis, horizontal long-axis, and vertical long-axis slice images obtained using a 3D OS-EM image reconstruction without motion compensation. Figures 1.7b and 1.8b show the corresponding images obtained using the 4D OS-EM image reconstruction with dual R&C motion compensation. They show the significant improvement in image quality in terms of improved image resolution from RM compensation and much lower image noise level from the CM compensation.

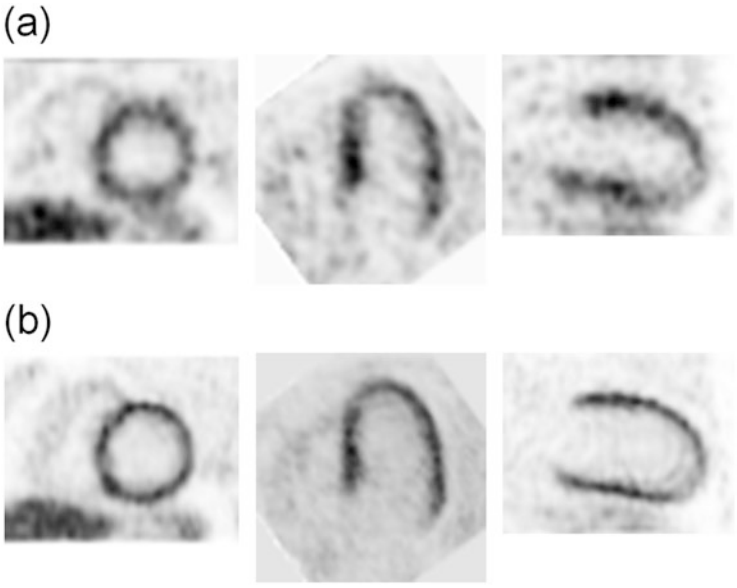

Fig. 1.7 (**a**) Sample images from one of the eight cardiac gates from selected sample (*Left*) short-axis, (*Middle*) horizontal long-axis, and (*Right*) vertical long-axis slices images obtained using a 3D OS-EM with no motion compensation from a $^{13}NH_3$ MP PET study. (**b**) Corresponding images obtained using the 4D OS-EM with R&C motion compensation

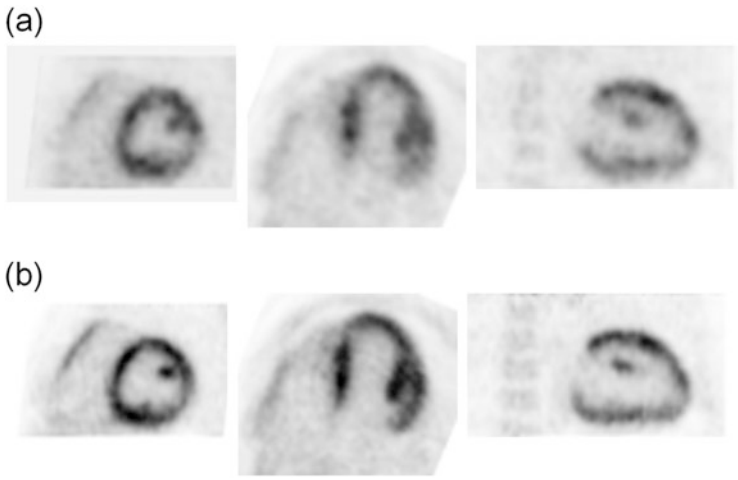

Fig. 1.8 (**a**) Sample images from one of the eight cardiac gates from selected sample (*Left*) short-axis, (*Middle*) horizontal long-axis, and (*Right*) vertical long-axis slices images obtained using a 3D OS-EM with no motion compensation from a ^{18}F-FDG cardiac PET study. (**b**) Corresponding images obtained using the 4D OS-EM with R&C motion compensation

1.4 Conclusions

Three-dimensional (3D) statistical image reconstruction methods using iterative algorithms and with models of the imaging physics and imaging system characteristics have shown to provide significant improvements in both the quality and quantitative accuracy of static SPECT and PET images. They have led to improved clinical diagnosis and, by trading off the improved image quality, for reduced patient dose and imaging time. In this work, we described newly developed 4D statistical image reconstruction methods that provided RM and CM compensation for further improvement in image quality and quantitative accuracy in PET images. We evaluated the effectiveness of the 4D image reconstruction methods using simulation and patient data.

Our results showed that a 4D image reconstruction method with RM and attenuation compensation provided quantitative lung PET images with reduced resolution loss due to RM blur and improved the detection of small lung lesions. We also evaluated a 4D image reconstruction method with dual R&C motion compensation using data from a clinical $^{13}NH_3$ MP PET and a clinical ^{18}F-FDG cardiac PET study. The results showed 4D gated cardiac PET images with improved image resolution from RM compensation and much lower image noise level from the CM compensation.

The improved 4D gated cardiac PET images reveal anatomical details, such as the papillary muscle and interventricular sulcus, of the heart that were not possible with conventional 3D image reconstruction methods. The anatomical details allowed the development of feature-based myocardial motion vector estimation methods [33, 34] that overcame the aperture problem in traditional motion

estimation methods. The accuracy of CM estimation will be further improved with continued improvement of the 4D image reconstruction methods and of the imaging characteristics in the next generation PET scanners that are coming into the market. It will allow extraction of new information about the contractility of the heart and provide additional diagnostic information for improved patient care.

References

1. Nehmeh SA, Erdi YE. Respiratory motion in positron emission tomography/computed tomography: a review. Semin Nucl Med. 2008;38(3):167–76.
2. Pretorius PH, King MA, Tsui BMW, LaCroix KJ, Xia W. A mathematical model of motion of the heart for use in generating source and attenuation maps for simulating emission imaging. Med Phys. 1999;26(11):2323–32.
3. McNamara JE, Pretorius PH, Johnson K, Mukherjee JM, Dey J, Gennert MA, et al. A flexible multicamera visual-tracking system for detecting and correcting motion-induced artifacts in cardiac SPECT slices. Med Phys. 2009;36(5):1913–23.
4. Chung A, Camici P, Yang G-Z, editors. List-mode affine rebinning for respiratory motion correction in PET cardiac imaging. Medical imaging and augmented reality. Berlin/Heidelberg: Springer; 2006.
5. Chen S, Tsui BMW. Evaluation of a new 4D PET image reconstruction method with respiratory motion compensation in a CHO study. J Nucl Med 2011: 150.
6. Chen S, Tsui BMW. Evaluation of a 4D PET image reconstruction method with respiratory motion compensation in a patient study. Society of nuclear medicine annual meeting. San Antonio; 2011: J Nucl Med. 2011. p. 2023.
7. Lee T-S, Higuchi T, Lautamäki R, Bengel F, Tsui BMW. Task-based evaluation of a 4D MAP-RBI-EM image reconstruction method for gated myocardial perfusion SPECT using a human observer study. Phys Med Biol. 2015;60:6789–809.
8. Lee T-S, Tsui BMW. Optimization of a 4D space-time gibbs prior in a 4D MAP-RBI-EMReconstruction method for application to gated myocardial perfusion SPECT. Proceeding of the fully three-dimensional image reconstruction meeting in radiology and nuclear medicine. 2009. p. 122.
9. Tang J, Lee T-S, He X, Segars WP, Tsui BM. Comparison of 3D OS-EM and 4D MAP-RBI-EM reconstruction algorithms for cardiac motion abnormality classification using a motion observer. IEEE Trans Nucl Sci. 2010;57(5):2571–7.
10. Tang J, Segars WP, Lee T-S, He X, Rahmim A, Tsui BMW. Quantitative study of cardiac motion estimation and abnormality classification in emission computed tomography. Med Eng Phys. 2011;33:563–72.
11. Gilland DR, Mair BA, Bowsher JE, Jaszczak RJ. Simultaneous reconstruction and motion estimation for gated cardiac ECT. IEEE Trans Nucl Sci. 2002;49(5):2344–9.
12. Mair BA, Gilland DR, Sun J. Estimation of images and nonrigid deformations in gated emission CT. IEEE Trans Med Imaging. 2006;25(9):1130–44.

13. Lee T-S, Tsui BMW. Evaluation of corrective reconstruction method for reduced acquisition time and various anatomies of perfusion defect using channelized hotelling observer for myocardial perfusion SPECT. IEEE nuclear science symposium and medical imaging conference record. 2010. p. 3523–6.
14. Dawood M, Buther F, Lang N, Schober O, Schafers K. Respiratory gating in positron emission tomography: a quantitative comparison of different gating schemes. Med Phys. 2007;34: 3067–6.
15. Klein GJ, Reutter BW, Ho MH, Reed JH, Huesman RH. Real-time system for respiratory-cardiac gating in positron tomography. IEEE Trans Nucl Sci. 1998;45:2139–43.
16. Chung A, Camici P, Yang G-Z. List-mode affine rebinning for respiratory motion correction in PET cardiac imaging. In: Medical imaging and augmented reality. Berlin: Springer; 2006. p. 293–300.
17. Büther F, Stegger L, Wübbeling F, Schäfers M, Schober O, Schäfers KP. List mode-driven cardiac and respiratory gating in PET. J Nucl Med. 2009;50:674–81.
18. Klein GL, Reutter BW, Huesman RH. Data-driven respiratory gating in list mode cardiac PET. J Nucl Med. 1999;40:113p.
19. Lamare F, Ledesma Carbayo MJ, Cresson T, Kontaxakis G, Santos A, Cheze Le Rest C, Reader AJ, Visvikis D. List-mode-based reconstruction for respiratory motion correction in PET using non-rigid body transformations. Phys Med Biol. 2007;52:[68].
20. Chen ST, Tsui BMW. Accuracy analysis of image registration based respiratory motion compensation in respiratory-gated FDG oncologcial PET reconstruction. In: IEEE nuclear science symposium & medical imaging conference. Dresden; 2008. p. M06-417.
21. Chen S, Tsui BMW. Four-dmiensional OS-EM PET image reconstruction method with motion compensation. In: Fully three-dimensional image reconstruction in radiology and nuclear medicine. Beijing; 2009. p. 373–6.
22. Li TF, Thorndyke B, Schreibmann E, Yang Y, Xing L. Model-based image reconstruction for four-dimensional PET. Med Phys. 2006;33:1288–98.
23. Qiao F, Pan T, Clark JW, Mawlawi OR. A motion-incorporated reconstruction method for gated PET studies. Phys Med Biol. 2006;51:3769–83.
24. Chen S, Tsui BMW. Joint estimation of respiratory motion and PET image in 4D PET reconstruction with modeling attenuation map deformation induced by respiratory motion. J Nucl Med. 2010;51(supplement 2):523.
25. Segars WP, Sturgeon G, Mendonca S, Grimes J, Tsui BMW. 4D XCAT phantom for multimodality imaging research. Med Phys. 2010;37(9):4902–15.
26. Segars WP. Development of a new dynamic NURBS-based cardiac-torso (NCAT) phantom, PhD dissertation, The University of North Carolina, May 2001.
27. Segars WP, Tsui BMW. MCAT to XCAT: the evolution of 4-D computerized phantoms for imaging research. Proc IEEE. 2009;97(12):1954–68.
28. Segars WP, Mori S, Chen G, Tsui BMW. Modeling respiratory motion variations in the 4D NCAT Phantom. In: IEEE medical imaging conference. 2007. p. M26-356.
29. Segars WP, Lalush D, Frey EC, Manocha D, King MA, Tsui BMW. Improved dynamic cardiac phantom based on 4D NURBS and tagged MRI. IEEE Trans Nucl Sci. 2009;56:2728–38.
30. Lewellen TK, Harrison RL, Vannoy S. The simset program. In: Monte Carlo calculations in nuclear medicine, Medical science series. Bristol: Institute of Physics Publication; 1998. p. 77–92.
31. Jan S, et al. GATE: a simulation toolkit for PET and SPECT. Phys Med Biol. 2004; 49(19):4543.
32. Shilov M, Frey EC, Segars WP, Xu J, Tsui BMW. Improved Monte-Carlo simulations for dynamic PET. J Nucl Med Suppl. 2006;47:197.
33. Wang J, Fung GSK, Feng T, Tsui BMW. A papillary muscle guided motion estimation method for gated cardiac imaging. In: Nishikawa RM, Whiting BR, Hoeschen C, editors. Medical imaging 2013: physics of medical imaging, Proc. of SPIE, vol. 8668. Washington: SPIE; 2013. p. 86682G.
34. Wang J, Fung GSK, Feng T, Tsui BMW. An interventricular sulcus guided cardiac motion estimation method. Conference record of the 2013 I.E. nuclear science symposium and medical imaging conference, Seoul, 2013;October 27–November 2. p. 978–84.